Applying machine learning to predict the impact of changing iron ore properties on blast furnace performance

T.R. Scott[1], C. Gous[1], J. Muller[1], and J.L. Deutsch[2]

[1]Anglo American, South Africa
[2]Resource Modeling Solutions, Canada

Value in use (VIU) properties include the physical and metallurgical iron ore properties that affect blast furnace operation. The physical and metallurgical variability associated with a lump iron ore product translates to changes in blast furnace production rates, operating costs and carbon emissions. Predicting these properties enables the appropriate management and marketing of the iron ore product, ensuring blast furnace customers receive ore within specification limits. However, a lack of geometallurgical data results in the common historic approach to assume that the lump ore properties of a deposit will be consistent year-on-year. This does not consider the expected geometallurgical variability and inhibits the proactive marketing of lump product.

This paper outlines a workflow that uses machine learning to incorporate sparse geometallurgical data on three VIU properties (tumble index, reducibility and reduction disintegration index) into a spatial model for an existing mine. This is done by relating these properties to primary geologic features that are included in the resource block model. The significance of developing a spatial geometallurgical model is demonstrated by predicting the impact of changing ore types on blast furnace carbon emissions.

INTRODUCTION

The iron- and steel-making industry is one of the highest carbon emission contributors from the industrial sector, contributing 7% of all the CO_2 emissions from the global energy system (International Energy Agency, 2020). Green steel initiatives, which aim to reduce this impact, can be grouped into two main categories: smart carbon usage (including carbon capture and storage) and carbon direct avoidance (including hydrogen-based reduction) (EUROFER, 2019). Many green steel-related projects focus on minimising or replacing the use of carbon in steelmaking (for examples, see Primetals Technologies, Ltd, 2021; Rechberger *et al.*, 2020; Suer *et al.*, 2021; Tonomura *et al.*, 2016). However, another crucial part of the 'iron ore + carbon + heat = steel' equation is the iron ore. This paper demonstrates the potential impact of changing lump iron ore properties on blast furnace (BF) carbon emissions by creating a spatial geometallurgical model of an existing iron ore deposit, predicting future ore properties and relating these to carbon impact during blast furnace-basic oxygen furnace (BF-BOF) steelmaking. In this way, scope 3 carbon emissions are estimated, which the Greenhouse Gas Protocol describes as all indirect emissions that occur up or downstream of a company's value chain.

Physical and Metallurgical Properties Affecting Blast Furnace Operation

The vast amount of research and investment in green steel, aligning with the 2015 Paris Agreement to reduce greenhouse gas emissions, indicates that controlling the amount of CO_2 released by blast furnaces will become increasingly important in the future. Blast furnaces largely rely on receiving primary iron ore with consistent metallurgical and physical properties, enabling smooth furnace operation and predictable emissions. Lump iron ore and pellets form a significant portion of blast furnace burden and may be used interchangeably (within operational limitations). Whilst iron ore pellets are well-known to exhibit fairly homogeneous properties, lump iron ore is more variable and often seen as unpredictable (Geerdes *et al.,* 2015). This variability has the potential to impact blast furnace operation and environmental impact. However, lump iron ore is environmentally favourable as it consumes less energy during its creation, compared to pellets and sinter. Additionally, lump iron ore often exhibits physical and metallurgical properties within similar ranges to that of pellet feed, as shown in Table I. Thus, the ability to predict and manage the physical and metallurgical properties of lump iron ore would eliminate the main disadvantage associated with its use.

Table I. Preferred metallurgical and physical properties for sinter, pellet and lump feed, (after Lu et al.*, 2015)*

	Units	Lump	Pellets	Sinter
TI (tumble index)	% +6.3mm	>80-85	>90	>65
AI (abrasion index)	% -0.5mm	<10	<3	<7
DI (decrepitation index)	% -6.3mm	<15	N/A	N/A
RDI (reduction disintegration index)	% -2.8mm	<25	N/A	<35
RI180 (reducibility index)	%	>60	>70	>65

The commonly measured physical and metallurgical (or geometallurgical) lump iron ore properties that impact blast furnace operation are described below.

Tumble and Abrasion Indices

The Tumble Index (TI, in % +6.3 mm) and Abrasion Index (AI, in % -0.5 mm) are physical properties determined with a standardised test (ISO3271), which characterises the degree of physical breakdown that can occur during handling and transportation. Fine material is typically screened from the product prior to loading the BF, which is necessary as the fines have a negative effect on BF burden permeability and gas flow. Consequently, the energy efficiency, fuel (coke) requirement, as well as hot metal productivity are affected. Higher TI properties result in the customer receiving less lump ore than expected. AI is indicative of the amount of -0.5 mm fines produced, which would be carried out with gas and lost as dust from the BF and directly affect hot metal productivity.

Reduction Disintegration Indices

Reduction-disintegration indices are physical properties which characterise the breakdown that occurs during the reduction of iron ore whilst transitioning from hematite to magnetite. Reduction-disintegration indices applicable to the BF are determined with a standardised test (ISO4696-1) as Reduction Disintegration Index -3.15 mm (RDI-3.15) and Reduction Disintegration Index -0.5 mm (RDI-0.5). The impact of RDI-3.15 in the BF-BOF process is due to the formation of fines and its negative effect on BF burden permeability, gas flow and effectively the energy efficiency and fuel (coke) requirement. It also influences hot metal productivity. RDI-0.5 is indicative of the amount of -0.5 mm fines produced, which would be carried out with gas and lost as dust from the BF and directly affect hot metal productivity.

Reducibility Indices

Reducibility indices are metallurgical properties indicative of the rate at which oxygen is removed during reduction of iron ore. The indirect reduction reactions that occur in the upper solid-state part of a BF have an overall lower energy demand per unit reduction compared to the direct reduction reactions that occur in the molten zone lower in the BF. The lower energy demand of indirect reduction reactions in the upper part of the BF generally implies a lower fuel (coke) requirement and CO_2 emissions for an ore with a higher reducibility, compared to an ore with a lower reducibility that will have more reduction occurring in the melting zone. The reducibility index considered indicative of the rate of reduction in the BF is determined with the standardised test (ISO7215) as the RI180. RI180 is the degree of reduction after 180 minutes of a 500g sample with size -20+18 mm being reduced with a mixture of CO and N_2 gases at 900°C.

SPATIAL MODELLING OF GEOMETALLURGICAL PROPERTIES

Incorporating geometallurgical properties into a spatial model presents several unique challenges, compared to the modelling of typical grade properties (Carrasco *et al.*, 2008), requiring specific workflows depending on deposit constraints. Options for spatially modelling geometallurgical variables (considering their non-additivity) include:

1. Geostatistical simulation (e.g. Avalos and Ortiz, 2019; Carrasco *et al*., 2008; Deutsch *et al*., 2016), which can be preluded by dimensionality reduction where many variables are to be modelled (e.g. Boisvert *et al.,* 2013). This stochastic option places no assumptions on variable additivity and has been shown to reasonably reproduce deposit variability. Additionally, this method can be used to model the joint uncertainty between variables.
2. Expressing geometallurgical variables as a function of additive properties (e.g. Adeli *et al.*, 2021; Lishchuk *et al*., 2019). Here, relationships are established between additive geological variables and non-additive geometallurgical variables. The additive variables are spatially estimated using methods such as kriging, after which a formula or machine learning (ML) model is applied to obtain a spatial estimate for the geometallurgical property. This method is deterministic and results in a single value for each block model cell; however, this method may not represent deposit variability as well as simulation.

Selection of which approach to follow should be based on the model purpose as well as the amount of data available for spatial modelling. The following outlines the method used to spatially model the geometallurgical properties of lump iron ore that influence BF carbon emissions.

METHODOLOGY

To spatially model the geometallurgical properties effecting CO_2 emissions (TI, RI180 and RDI-3.15), data from an operational iron ore mine were examined. The geometallurgical samples are collected as part of a dedicated geometallurgical core drilling program and subjected to test work meeting ISO3271 (TI), ISO7215 (RI180) and ISO4696-1 (RDI-3.15) standards. Only lump hematite ore of Direct Shipping Ore (DSO) grade were submitted for the test work. Other data on these samples include chemistry, lithology, core competency and ore textural data. A total of 453 composite results were available, which were representatively spaced across the ore deposit as well as across the various ore textures to be mined.

Although a fair amount of geometallurgical samples exists for the operation, there is insufficient data density to establish variograms or perform geostatistical simulation. Considering the availability of resource models with spatially estimated chemistry, lithology and ore textural data; the next option is to investigate the relationship between these modelled properties and geometallurgical variables. Upon establishment of these relationships, an algorithm can be applied to each cell of the resource block model to derive estimates of the geometallurgical variables.

Decision tree-based machine learning (i.e. random forest and gradient boosting regression) was used to investigate these relationships as they have been shown to reliably model the non-linear relationships between metallurgical variables and primary geological properties, particularly where data is sparse (Jooshaki *et al*., 2021; Khushaba *et al.,* 2022; Lishchuk *et al*., 2019). Whilst neural network methods have also been shown to perform well (Both and Dimitrakopoulos, 2021; Gholami *et al*., 2022; Mena Silva *et al.*, 2020), these typically require large amounts of data and are more difficult to interpret, and thus were not used in this study. As the chemistry variables have been estimated using ordinary kriging, the result will be a deterministic estimate of the geometallurgical properties. Some degree of smoothing is expected, however this is adequate considering the purpose of the model is to understand the long term impact of changing ore properties on blast furnace performance.

Development of the Machine Learning Model

The machine learning workflow was developed using the Resource Modelling Solutions Platform. The data preparation steps that preluded ML includes a thorough exploratory data analysis, unfolding of coordinates and data imputation. Chemistry data were input as continuous variables whilst texture, competency and geographic sublocation were input as categorical variables. These properties were iteratively run on a random forest machine learning model to predict the geometallurgical response variable; subtracting the least important predictor from the model with each iteration. Where a significant drop in R^2 or route mean squared error occurred, the previously removed predictor was re-introduced to create the final list of optimised predictors.

Once an optimised set of predictor variables were established, the ML models were iteratively tuned to achieve an optimised set of hyperparameters. Both random forest and gradient boosting regressor models were trialled for each property. For more information on scalable tree boosting systems and associated hyperparameter optimisation, the reader is referred to Chen and Guestrin (2016).

A common approach when developing ML models is to withhold a portion of the dataset from training (i.e. the validation set) and use this to test the final model. Due to the limited data available, all data was used during model training to achieve as accurate a model as possible, which was then tested with K-fold validation. As the geometallurgical programme continues, future results can be used to test the accuracy of the current model and refine where necessary.

Machine Learning Results

The optimised models for TI, RI180 and RDI-3.15 are displayed in Figure 1. The scatterplot on the left shows the actual versus predicted values when all composite data is used to both fit and test the model. The scatterplot on the right shows the machine learning results when portions of the data are iteratively set aside and used to test the model through K-fold validation. Decreased model performance is expected when portions of the data are withheld as tests, however one would not want to observe a significant bias between the models on the left and right. A significant difference in the shape and statistics of the scatterplots on the left and right would indicate overfitting of the ML model. Although the R^2 values of test models are <0.5, this is considered relatively good in view of the complexities of geometallurgical data. All three of the models displayed are considered reasonable for the prediction of the geometallurgical properties, with the RI180 model showing the best performance.

Feature importance plots (which rank the variables used in the ML models according to their importance when predicting the response) as well as partial dependence plots were used to discuss the geological drivers of geometallurgical properties. The final list of predictors consists of a suite of elements (included as continuous variables) as well as one categorical variable that denotes whether the sample originates from a specific pit on the mine. The geometallurgical properties of this area are significantly different to the rest of the mine and warrant inclusion as a binary indicator in the ML models.

Geological Interpretation of Machine Learning Predictors

The feature importance plots yielded from machine learning are a useful tool in understanding the geological properties driving geometallurgical response. Although individual predictors are at times strongly correlated with the response variable, these bivariate relationships may not adequately account for response variability. This is where machine learning, which uses multiple predictor variables that may be linearly or non-linearly correlated with the response, is powerful in predicting geometallurgical properties. For example, textural differences play a large role in determining RI180, RDI-3.15 and TI. However, hydrothermal alteration of laminated ore may result in reducibility values resembling massive ore. This results in an overlap in the RI180 properties between these two textures that are difficult to distinguish through bivariate or linear relationships.

Each variable used in predicting the response was geologically justified. This was done to improve confidence in the ML models and flag any predictors that don't pass a 'logic-check'. The main predictors used in the ML models are:

- RI180 and RDI-3.15: the binary variable representing whether the sample originates from a specific pit, BaO (present in baryte), Al_2O_3 (likely present in muscovite crystals), CaO (present in calcite veins) and phosphorous (present in apatite).
- Tumble Index: CaO, loss on ignition (LOI), phosphorous and Al_2O_3

The geological properties interpreted as driving these predictors (and thus the geometallurgical response) include ore texture, mineralogy, hydrothermal alteration, and structural complexity.

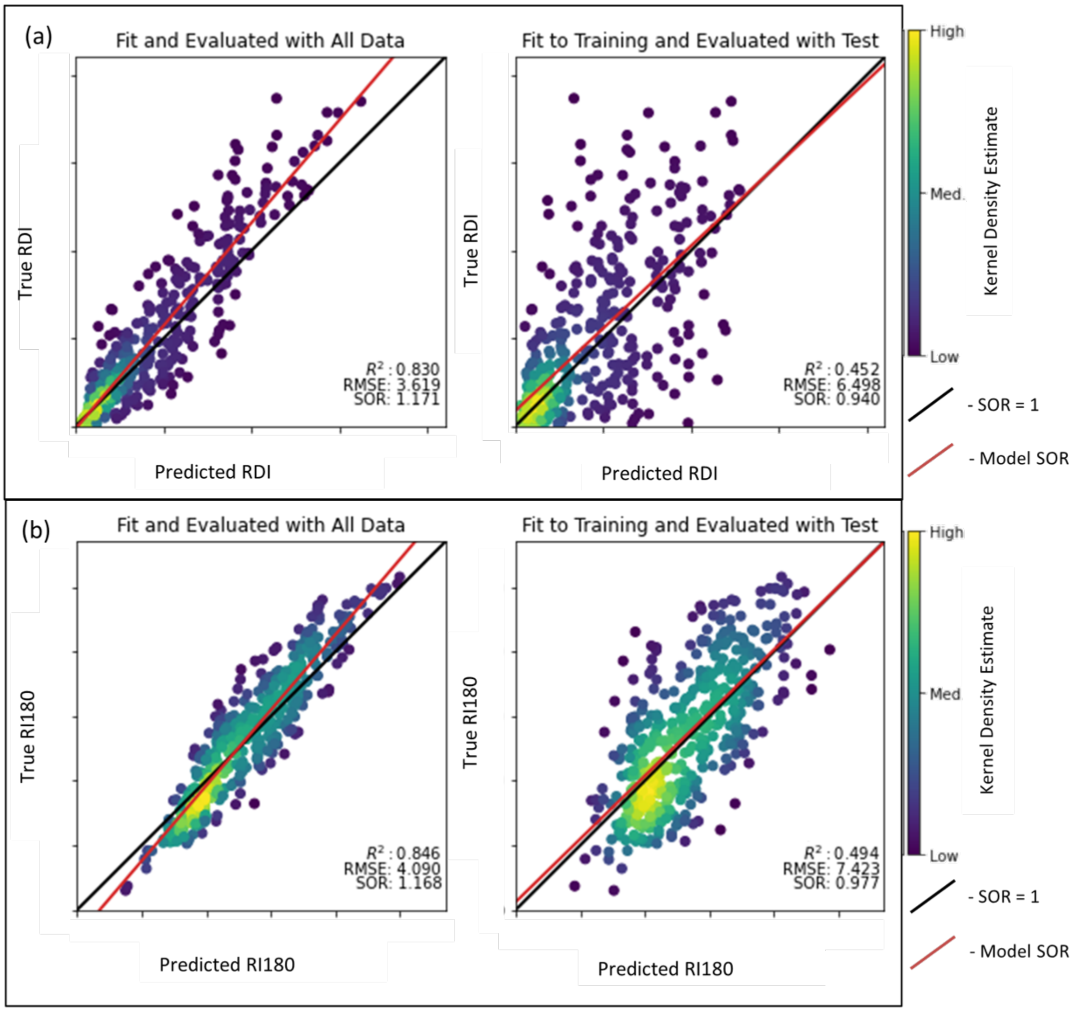

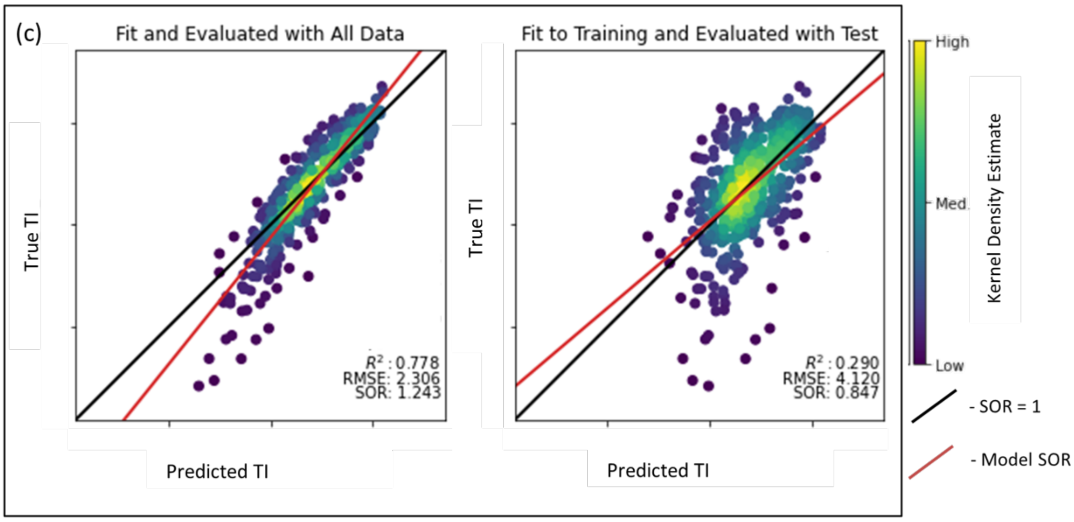

Figure 1. Machine learning models for (a) RDI-3.15, (b) RI180 and (c) TI, coloured by the relative density of data points. SOR: slope of regression.

The Influence of Ore Texture on Geometallurgical Properties

Differences in geometallurgical properties per ore texture are evident from the cumulative distribution function plots in Figure 2. However, the chemistry variation across each texture is expected to account for the property variations, negating the need for textures as categorical indicators in the ML models. Despite excluding textural features in the ML models, textural controls on properties such as RI180 and RDI-3.15 are evident in the resulting block model (discussed later). Areas that are known to exhibit laminated textures show different RI180 and RDI-3.15 properties from massive textures. Laminated ore contains slightly higher porosity levels, with more discontinuities that would facilitate the penetration of reducing gases in the blast furnace, leading to higher RI180 values. Massive ore exhibits improved RDI-3.15 properties. This is thought to be due to the higher bond strengths, but further work is needed to confirm this theory.

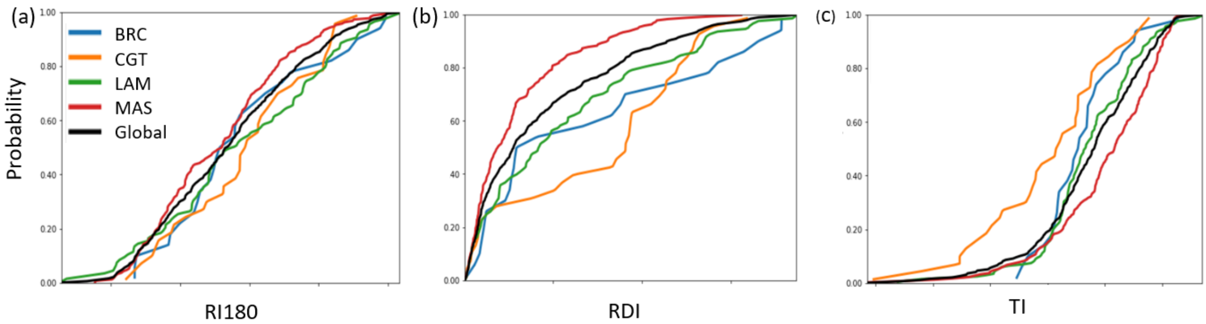

Figure 2. Cumulative distribution function plots for (a) RI180, (b) RDI-3.15 and (c) TI, separated according to ore texture. BRC: brecciated, CGT: conglomeratic, LAM: laminated, MAS: massive.

Spatial modelling of TI, RI180 and RDI-3.15

Not all the required predictors are currently estimated in the resource block model. As such, the ML models developed during this study were re-run using only the predictors that are included in the existing resource model. The resulting ML models are less accurate but still considered reasonable for predictions. These ML models have been applied to the resource block model to gain an understanding of the spatial variation in geometallurgical properties for the mine.

Spatial Model Results

The spatial geometallurgical estimates were subjected to a visual check; the results of which align with current knowledge of the deposit and are geologically reasonable (see Figures 3, 4 and 5). As mentioned previously, the RI180 and RDI-3.15 block model results correlate with areas known to exhibit laminated and massive ore textures, validating these estimates. Areas that historically exhibited harder ore during mining are also correlated with higher TI values.

Data reproduction plots were created to compare each geometallurgical sample result with the encapsulating cell estimate. Reasonable data reproduction is observed. The general CDF shapes are well-reproduced, with block model variability showing slightly less variability than that observed on the sample scale.

Several benefits have been demonstrated through the machine learning exercise in this study. Firstly, no explicit domaining is required beyond the use of DSO-grade (i.e. >61.0% Fe) ore samples. Chemical controls on ore textures have been detected by the machine learning algorithm and is evidenced by the spatial correlation between RI180, RDI-3.15 and ore textures. Thus, textural data was not required as an input to the ML model. Additionally, geographical sub-location was input as a categorical indicator, negating the need to separately analyse the data per area.

Secondly, application of the ML model to chemistry estimates of the block model does not impose any assumptions on the additivity of the geometallurgical properties. As these properties are non-additive, averaging should always be delayed as long as possible to minimise potential model biases. For example, when calculating average metallurgical properties for a specific volume, the average chemistry should be calculated, and the ML model subsequently applied to the averaged chemistry results. Fully quantifying the additivity constraints of TI, RI180 and RDI-3.15 would enable more accurate results in future model updates.

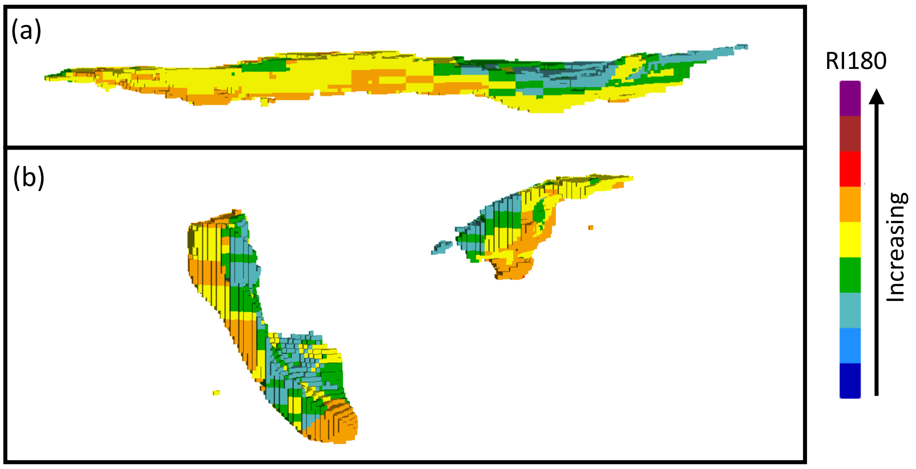

Figure 3. Ore body cross sections showing spatial variability in RI180.

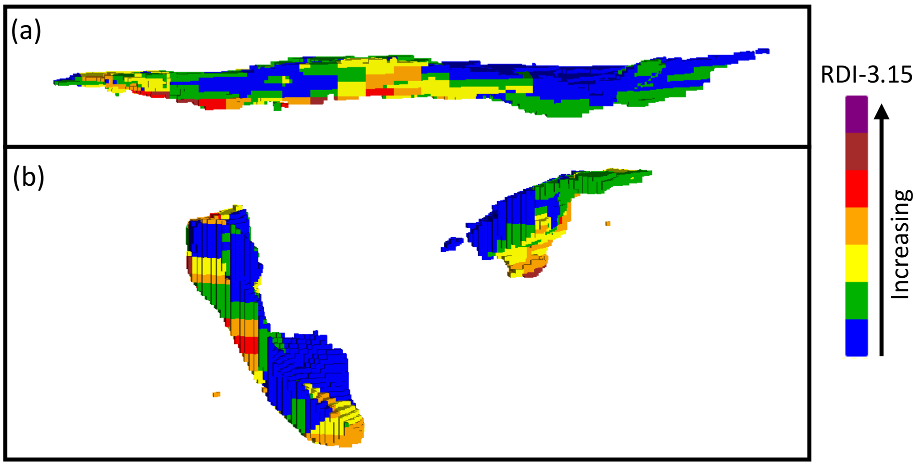

Figure 4. Ore body cross sections showing spatial variability in RDI-3.15.

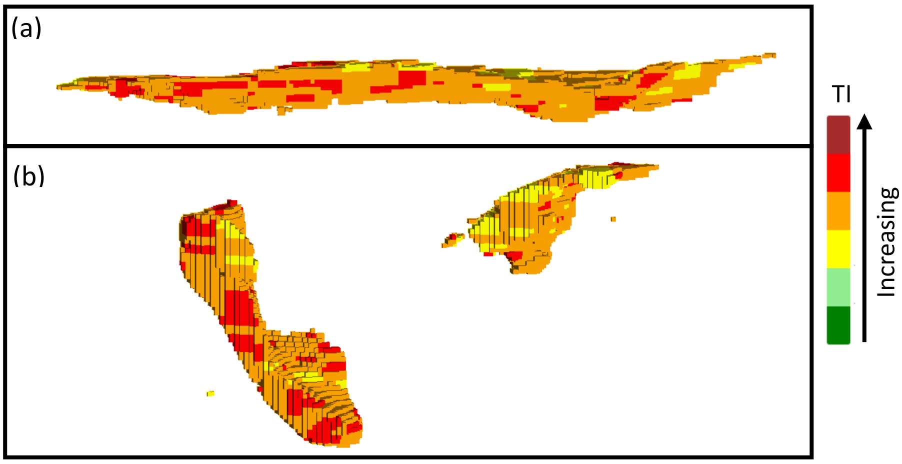

Figure 5. Ore body cross sections showing spatial variability in TI.

The main limitations associated with the spatial model include the smoothed block model result (due to the application of ML models to kriged chemistry estimates). As such, the model should not be used to assess local or small-scale variability. The variability and local accuracy of future model updates is expected to improve through the inclusion of all important predictor variables in the resource block model.

There is no quantification of the joint uncertainty between variables, and no direct control on the spatial relationships between geometallurgical properties. Within this modelling workflow, it is assumed that assay data accounts for these spatial relationships and this assumption is validated by post-model checks. However, as more geometallurgical data is collected, techniques such as decorrelation followed by sequential gaussian simulation may provide better controls on multivariate relationships in future.

NON-SPATIAL MODELLING OF THE CO_2 IMPACTS OF CHANGING GEOMETALLURGICAL IRON ORE PROPERTIES ON THE BF-BOF STEELMAKING ROUTE

To use the spatial geometallurgical model to forecast the impact that changing ore properties have on BF carbon emissions, a non-spatial model was developed. This model calculates the ΔCO_2 per incremental change in TI, RI180 and RDI-3.15. The development of this model is explained below.

The impacts of varying iron ore properties in a particular steel-making process are considered in terms of the total direct and indirect CO_2 emissions. To determine the CO_2 emissions impact of iron ore properties, a techno-economic model of the relevant steelmaking process route is used. These models employ mass- and energy-balances, and other sub-models incorporating the fundamental relationships relating iron ore properties to operating parameters, which directly impact the CO_2 emissions.

The CO_2 emissions impacts are determined of an ore relative to the specification of another ore, deriving from the differences in properties of the two ore specifications. The change in CO_2 emissions of the steel-making process indicates the difference when 1 ton of ore is substituted with the other.

Application of the process models to calculate the CO_2 emissions impacts of an ore relative to another is illustrated in Figure 6. The process model of the relevant steelmaking route is configured with operating parameters and constraints for either a specific plant of a steel producer (ore consumer), or for example a typical steel producing market segment. The base model scenario has specified as input the iron ore being compared to, specified in terms of its chemical, physical, and metallurgical properties. The alternative model scenario is setup with the same parameter values but has an amount of the base ore substituted with the alternative iron ore. The base and alternative model scenarios are calculated to the same operating parameter values and constraints, and the differences calculated between the model of total direct and indirect CO_2 emissions. These differences in CO_2 emissions are divided by the amount of base ore replaced with the alternative ore to yield the specific values (per ton ore replaced) for ΔCO_2.

Typically, the RI180 of an ore at its actual particle size is considered in conjunction with softening and melting temperatures, determined in the standardised high-temperature BF simulation test (REAS test). A 'Reduction at Softening' (Rs) value is estimated for an ore that represents the degree of reduction at softening, which is the property entered into the BF model, impacting the reductant rate and metal productivity.

With regards to TI, model calculations relate to the physical breakdown within the blast furnace and the negative effect of resulting fines on the burden permeability. The percentage fines screened out before the BF, and the percentage fines left over in the BF feed are both explicitly specified, which required estimation thereof from the particle size distribution (PSD) at load port, estimation of the amount of handling and transportation to a specific steel mill and correlation between TI and degradation.

The model is applied to determine the incremental CO_2 emissions impact of each relevant iron ore property, e.g. determining what is the ΔCO_2 of only the difference in reducibility from the base ore to that of the alternative ore, and for the difference in Fe-content, etc. The base and alternative scenarios are initially setup both with the properties of the base ore, and then the properties in the alternative scenario are changed one at a time, and the alternative scenario model calculated.

CO_2 emissions impact values

The specific CO_2 emissions impacts were determined with BF-BOF steel making model (Table II), listed as ΔCO_2 impact values for each ore property per unit change between the base and alternative ore properties. For example, replacement of an ore with another having a Tumble Index (TI) that is 1% higher, implies a decrease in CO_2 emissions of 2.9 kg CO_2 for every ton of ore replaced.

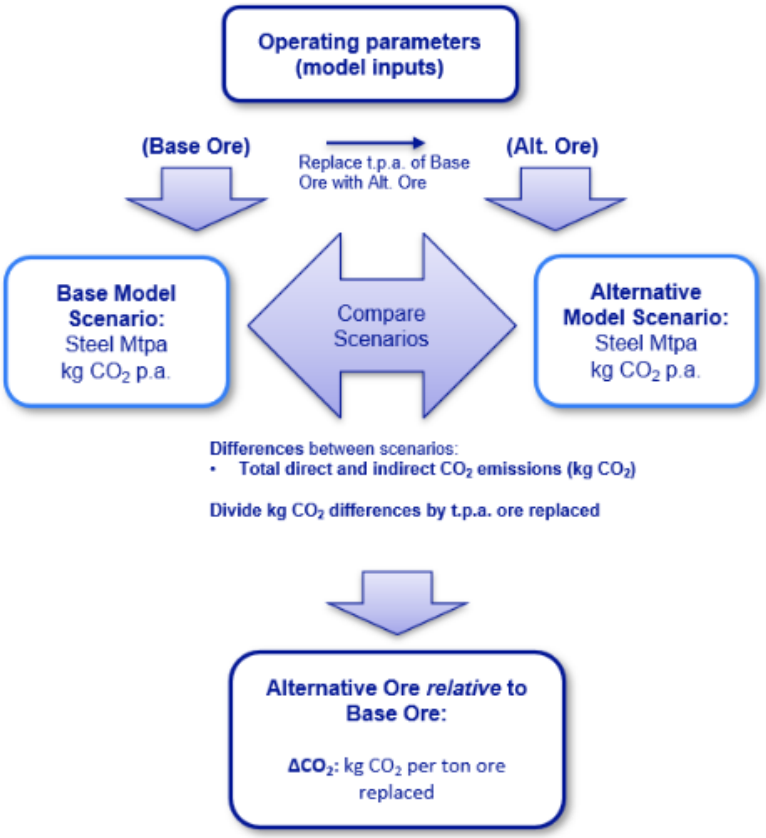

Figure 6. Modelling VIU and CO2 emissions impacts of an alternative ore relative to a base ore.

To note, the CO_2 impacts listed in Table II are for each property considered independently of each other, and only for the change in that property alone, assuming that all other properties remain unchanged. For example, the impacts listed for Fe(tot) are only for the change in Fe-content, assuming that the gangue components (SiO_2, Al_2O_3) are unchanged, and that the impacts of changes in the gangue components will be calculated separately.

RELATING THE SPATIAL ORE PROPERTIES TO CO_2 IMPACTS

The information shown in Table 2 indicates the CO_2 impact for the percentage change in each geometallurgical and chemical property. This information can be applied to block model forecasts, which include chemistry and geometallurgical property predictions. In this way, changes in scope 3 carbon emissions can be estimated according to actual fluctuations in ore properties. Figure 7 shows the impact of changing ore properties for the mine, between year 'x' and year 'x+1', on CO_2 emissions during blast furnace operation. Al_2O_3, although only displaying slight fluctuations year-on-year, is the predominant feature affecting ΔCO_2 emissions during the two years under investigation. Considering the geometallurgical properties, RI180 (which is influenced by ore texture, structural complexity and hydrothermal alteration) has the highest impact on CO_2 emissions.

Table II. Specific CO_2 impacts per unit property of iron ore in the BF-BOF steel making route

Iron Ore Property	Property Unit for Impact	Description	Primary Impact (for property increase)	ΔCO_2, $kgCO_2$/dmt/unit
TI (ISO3271)	1%>6.3 mm	Tumble index (TI), includes effect of Abrasion Index (AI) expected opposite change.	Decrease in -6.3 mm and -0.5 mm fines generation, burden permeability improvement, lower dust losses. Lower coke rate, increased productivity.	-2.90
RDI-3.15 (ISO4696-1)	1%<3.15 mm	Reduction disintegration index (-3.15 mm fraction), includes effect of RDI-0.5 expected change.	Increase in -3.15 mm and -0.5 mm fines generation during reduction, lower burden permeability, more dust losses. Increased coke rate, decreased productivity.	1.08
RI180 (ISO7215)	1% Reduction	Reducibility index RI180 determined by ISO7215 and adjusted for particle size.	Increased degree of indirect reduction – lower energy requirement. Lower coke rate, increased productivity.	-3.77
Fe(tot)	1% Fe(tot)	Total Fe-content	Increased productivity / lower specific ore requirement.	-5.51
SiO_2	1% SiO_2	SiO_2-content	Increase in slag SiO_2 and decrease in Al_2O_3. Saving in Quartz for controlling slag Al_2O_3.	-1.90
Al_2O_3	1% Al_2O_3	Al_2O_3-content	Increase in slag Al_2O_3. Increase in Quartz required to control slag Al_2O_3.	112.29
K_2O	1% K_2O	K_2O-content	Increase in alkali-loading. Decrease in coke reactivity and increased coke rate, and/or decrease in slag basicity and increased Sulphur removal costs.	116.2

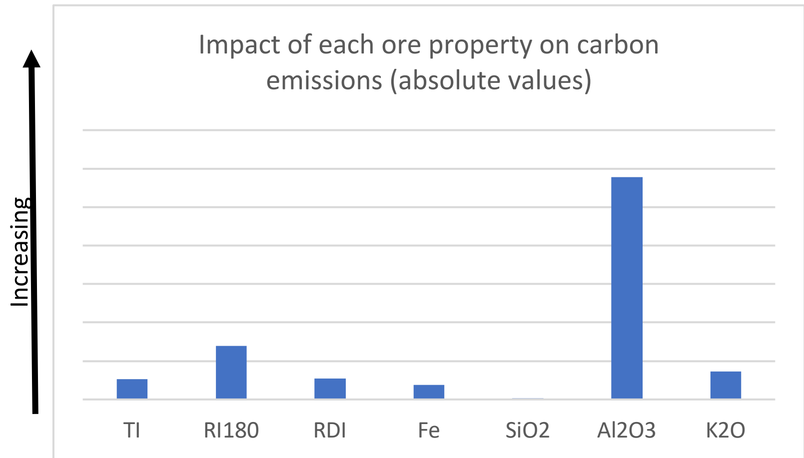

Figure 7. Impact of each ore property on carbon emissions, from year x to year x+1.

Relative to the baseline CO_2 emissions expected during blast furnace operation, this year-on-year change in ore properties impacts total blast furnace emissions by 5.3%. This includes changing Al_2O_3 contents that impact total blast furnace emissions by approximately 3.33%, and the change in RI180 that affects emissions by a further 0.80%. This provides one brief example of the effect that short term changes in ore properties have on blast furnace operation.

CONCLUSION

To support sustainable human development whilst minimising impact on the environment, several 'green steel' initiatives are being developed across the industry. Many of these initiatives focus on the DRI-EAF steel making route which uses natural gas or hydrogen to reduce primary iron ore. The use of renewable energy sources offers potential for further reductions in CO_2 emissions. However, until the industry can make a complete transition towards new and innovative solutions, the use of existing commercial blast furnaces continues to play a significant role in the short to medium term.

Although the environmental impacts during the various stages of BF-BOF steel making are well understood, the effects of changing ore properties have not been well-documented. Variability in ore properties is of particular importance where lump iron ore is fed into the blast furnace. The lower processing needs of lump ore, compared to pellet and sinter feed, make it a favourable product from a carbon emissions perspective. However, lump iron ore is prone to higher variability in chemical, physical and metallurgical properties; all of which influence blast furnace efficiency.

This study uses machine learning to incorporate sparse geometallurgical data into a spatial model for the mine. Although there are use limitations due to the smoothing of estimates, the model can be used to predict yearly changes in the geometallurgical ore properties that affect blast furnace CO_2 emissions. Applying the model to forecast a year-on-year change in ore properties showed that varying Al_2O_3 and RI180 properties had the highest impact on CO_2 emissions. Total ore properties caused a relative change of 5.3% in the CO_2 emissions of a typical blast furnace. This demonstrates the effect of changing geological properties on carbon emissions, and thus the need for thorough ore characterisation. A robust understanding of future lump iron ore properties is important to gain the most out of blast furnace optimisation efforts.

REFERENCES

Adeli, A., Dowd, P., Emery, X., Xu, C. (2021). Using cokriging to predict metal recovery accounting for non-additivity and preferential sampling designs. *Minerals Engineering*, 170, 106923.

Avalos, S., Ortiz, J.M. (2019). A simple, synthetic and two dimensional geometallurgical modeling application. Annual Report 2019. Predictive Geometallurgy and Geostatistics Lab, Queen's University.

Boisvert, J.B., Rossi, M.E., Ehrig, K., Deutsch, C.V. (2013). Geometallurgical Modeling at Olympic Dam Mine, South Australia. *Mathematical Geosciences*, 45, 901–925.

Both, C., Dimitrakopoulos, R. (2021). Applied Machine Learning for Geometallurgical Throughput Prediction—A Case Study Using Production Data at the Tropicana Gold Mining Complex. *Minerals,* 11(11), 1257.

Carrasco, P., Chilès, J.-P., Séguret, S.A. (2008). Additivity, metallurgical recovery, and grade. *In 8th International Geostatistics Congress,* Santiago, Chile.

Chen, T., Guestrin, C. (2016). XGBoost: A scalable tree boosting system. *In Proceedings of the 22nd ACM SIGKDD international conference on knowledge discovery and data mining*, pp 785-794.

Deutsch, J.L., Palmer, K., Deutsch, C.V., Szymanski, J., Etsell, T.H. (2016). Spatial Modeling of Geometallurgical Properties: Techniques and a Case Study. *Natural Resources Research*, 25, 161–181.

EUROFER (2019). Low Carbon Roadmap, Pathways to a CO_2-neutral European steel industry. https://www.eurofer.eu/assets/Uploads/EUROFER-Low-Carbon-Roadmap-Pathways-to-a-CO2-neutral-European-Steel-Industry.pdf [accessed 18 January. 2023].

Geerdes, M., Chaigneau, R., Kurunov, I., Lingiardi, O., Ricketts, J. (2015). *Modern Blast Furnace Ironmaking - an introduction*, Third. ed. IOS Press BV, Amsterdam, Netherlands.

Gholami, A., Asgari, K., Khoshdast, H., Hassanzadeh, A. (2022). A hybrid geometallurgical study using coupled Historical Data (HD) and Deep Learning (DL) techniques on a copper ore mine. *Physicochemical Problems of Mineral Processing*. 58(3), 147841.

International Energy Agency (2020). Iron and Steel Technology Roadmap. https://www.iea.org/reports/iron-and-steel-technology-roadmap [accessed 19 January. 2023].

Jooshaki, M., Nad, A., Michaux, S. (2021). A Systematic Review on the Application of Machine Learning in Exploiting Mineralogical Data in Mining and Mineral Industry. *Minerals*. 11(8), 816.

Khushaba, R.N., Melkumyan, A., Hill, A.J. (2022). A Machine Learning Approach for Material Type Logging and Chemical Assaying from Autonomous Measure-While-Drilling (MWD) Data. *Mathematical Geosciences*. 54(2), 285–315.

Lishchuk, V., Lund, C., Ghorbani, Y. (2019). Evaluation and comparison of different machine-learning methods to integrate sparse process data into a spatial model in geometallurgy. *Minerals Engineering*. 134, 156–165.

Lu, L., Pan, J., Zhu, D. (2015*). Quality requirements of iron ore for iron production, in: Iron Ore Mineralogy, Processing and Environmental Sustainability*. Woodhead Publishing Series, Elsevier, United Kingdom, pp. 475–504.

Mena Silva, C.A., Ellefmo, S.L., Sandøy, R., Sørensen, B.E., Aasly, K. (2020). A neural network approach for spatial variation assessment – A nepheline syenite case study. *Minerals Engineering*. 149, 106178.

Primetals Technologies, Ltd. (2021). HYFOR pilot plant under operation - the next step for carbon free, hydrogen-based direct reduction is done. https://www.primetals.com/press-media/news/hyfor-pilot-plant-under-operation-the-next-step-for-carbon-free-hydrogen-based-direct-reduction-is-done [accessed 18 January. 2023].

Rechberger, K., Spanlang, A., Conde, A.S., Wolfmeir, H., Harris, C. (2020). Green Hydrogen-Based Direct Reduction for Low-Carbon Steelmaking. *Steel Research International*. 91(11), 2000110.

Suer, J, Traverso, M., Ahrenhold, F. (2021). Carbon footprint of scenarios towards climate-neutral steel according to ISO 14067. *Journal of Cleaner Production*. 318, 1–12.

Tonomura, S., Kikuchi, N., Ishiwata, N., Tomisaki, S., Tomita, Y. (2016). Concept and current state of CO_2 ultimate reduction in the steelmaking process (COURSE50) aimed at sustainability in the Japanese steel industry. *Journal of Sustainable Metallurgy*. 2(3), 191–199.

Tricia Robyn Scott

Specialist Geometallurgist
Anglo American

Tricia Scott is a Specialist Geometallurgist at Anglo American. Her role involves providing geometallurgical support to several operations across the globe, with a focus on geometallurgical modelling and estimation. She has over a decade of experience working on iron ore deposits and has assumed various geological roles at both active operations and exploration sites.

Her MSc(Eng), completed in 2021, focused on the geometallurgical properties of lump iron ore that effect blast furnace operation. She finds great fulfillment in characterizing rocks to optimise the processes that depend on them. In a rapidly evolving industry, Tricia believes that a comprehensive understanding of our geological resources is the bedrock for achieving business, environmental and strategic goals.